International Journal on Advanced Science Engineering Information Technology

Vol.15 (2025) No. 2
ISSN: 2088-5334

Development of an Internet of Things-Based Water Quality Monitoring System for Shrimp Ponds Utilizing Mappi32

Herlinawati [a,b,*], Afri Yudamson [a], Sri Ratna Sulistiyanti [a], Muhammad Ifan Saputra [a], Bagus Hendrawan [a]

[a] *Department of Electrical Engineering, University of Lampung, Lampung, Indonesia*
[b] *Doctoral Program in Environmental Science, University of Lampung, Lampung, Indonesia*
Corresponding author: [*]herlinawati@eng.unila.ac.id

Abstract*—Indonesia's vast waters make its aquatic resources abundant, with one of the most valuable resources being *Vannamei* shrimp. Technology-based shrimp farming is an essential method for utilizing this resource. Maintaining optimal water quality parameters is necessary for successful shrimp farming, as it affects shrimp breeding. Ideal conditions for shrimp breeding include a temperature range of 26-32°C, salinity of 30-35 ppt, pH of 7.6-8.3, turbidity of 11-24 NTU, and oxygen levels of more than 4 mg/L. This research integrates sensors for real-time shrimp pond water quality monitoring using Internet of Things (IoT) technology, with sensors calibrated for error rate and accuracy. The error rates of the sensor testing process are TDS sensor 5.39%, temperature sensor 0.14%, pH sensor 2.85%, turbidity sensor 5.14%, and DO sensor 8.84%. This research successfully monitored the water quality of shrimp ponds in real-time through the Node-Red dashboard with the MQTT IoT protocol and an average latency of 593.3 ms. Over ten days, the average water quality parameters were as follows: in the morning salinity 31.86 ppt, temperature 27.13°C, pH 7.66, turbidity 17.24 NTU, and dissolved oxygen 5.22 mg/L; in the afternoon salinity 31.69 ppt, temperature 27.41°C, pH 7.84, turbidity 17.24 NTU, and dissolved oxygen 5.54 mg/L; and at night salinity 31.90 ppt, temperature 27.35°C, pH 7.78, turbidity 17.21 NTU, and dissolved oxygen 5.36 mg/L. Further research is needed to implement the Fuzzy Logic method to determine the optimal status of shrimp pond water and evaluate the effectiveness of the process on the control system.

***Keywords*— Monitoring; shrimp ponds; Mappi32; Internet of Things (IoT); Message Queuing Telemetry Transport (MQTT).**

Manuscript received 15 Oct. 2020; revised 29 Jan. 2021; accepted 2 Feb. 2021. Date of publication 30 Apr. 2025.

I. INTRODUCTION

The Unitary State of the Republic of Indonesia, or NKRI, is the largest archipelago in the world [1], [2]. This archipelagic state means a country has many islands united by territorial waters. The 1982 UNCLOS Convention on the Law of the Sea supports this statement by discussing several points related to the sea law for archipelagic states [2]. The law of the sea states that the state has the right to establish its territorial sea zone up to 12 nautical miles from the coastal baseline. The state also has the right to establish an exclusive economic zone up to 200 nautical miles from the coastline and exploit and conserve natural resources, such as underwater fish, oil, and the continental shelf. This makes Indonesia an archipelago that can utilize the living resources in its waters [3].

Indonesia's aquatic resources are very abundant because of its vast waters. One type of resource in the Indonesian Sea with a high selling value is shrimp (*Vannamai*) [4]. Shrimp is a prime product in fisheries because it has economic value and promising export prospects [5]. Cultivating in ponds is one way to utilize shrimp in Indonesia [6]. The cultivation will play an essential role in producing data on monitoring the water quality of shrimp ponds [7]. The data is one of the most critical aspects of the decision-making process [8].

Shrimp pond farming must pay attention to the value of water quality parameters. This will affect the breeding of shrimp. The pond water quality parameters include the temperature, salinity, pH, oxygen levels, and turbidity in the shrimp pond water [9],[10]. The optimal parameters used in supporting shrimp breeding are temperature values of 26-32 ° C, salinity 30-35 ppt, pH 7.6-8.3, turbidity values of 11-24 NTU, and oxygen levels > 4 Mg / L [11]. These parameters can be measured using sensors validated for their readings [12]. The process of testing sensors that do this validation will be compared with calibrated conventional measuring instruments. Sensors are standardized to ensure shrimp breeding goes well.

The sensors will be integrated with Internet of Things (IoT)-based digitalization technology to support shrimp pond water quality monitoring [12]. IoT is a device that can receive

and send data in a network without human-to-human or human-to-computer interaction [13]. IoT can monitor the measured values on sensors. IoT technology will provide effective and efficient solutions to support the success of shrimp farming [14].

The communication protocol used to implement IoT in monitoring systems is Message Queuing Telemetry Transport (MQTT). MQTT is a machine-to-machine (M2M) and lightweight message [15]. This protocol uses the publish/subscribe communication method [16]. MQTT messages are sent to the broker and contain topics sent by the Publisher. The use of MQTT in IoT devices was chosen because this protocol requires much less energy consumption than other protocols. MQTT can also function well in a small bandwidth and high latency environment [17]. The latency indicates the time required for the data transmission process from the sender to the receiver [18].

Therefore, this research aims to integrate sensor monitoring of shrimp pond water quality into a system that can retrieve measurement data in real time and acquire sensor measurement data into a simple dashboard using the Message Queuing Telemetry Transport (MQTT) protocol based on the Internet of Things.

This research only makes a prototype of a shrimp pond water quality monitoring tool that can read the parameters of temperature, salinity, turbidity, oxygen levels, and pH. Then, data collection is carried out in an aquarium using water samples that have been conditioned, such as pond water. Then, the water sample will be treated by adding salt, detergent, and rainwater to see the response of the automatic treatment designed on the shrimp pond water quality monitoring system. Furthermore, this research only discusses sending sensor data to the Internet of Things system.

II. Materials and Methods

Mappi32 is an Internet of Things (IoT) development board designed and produced by KMTek (Karya Merapi Teknologi) company in Indonesia. The Mappi32 can be a microcontroller with functions similar to the Arduino development board. As a microcontroller, Mappi32 can work as an input controller in the form of sensors, collecting data from various sensor inputs and processing them. Mappi32 is a microcontroller with a CPU base, namely ESP32-WROOM-32E. In addition, mappi32 can work with a voltage output of 3-5V with LoRa, Wi-Fi, and Bluetooth support systems [18].

Total dissolved solids (TDS) refer to inorganic salts and small quantities of organic matter in water. The main components typically include cations such as calcium, magnesium, sodium, and potassium, and anions like carbonate, bicarbonate, chloride, sulfate, and nitrate [19]The salinity sensor's measurement results are in Parts per Million (PPM) or Parts per Trillion (PPT), or part per one million of the number of dissolved particles.

The DS18B20 sensor measures temperature by converting thermal energy into voltage and current. Uniquely, this sensor can be made parallel to one input [20]. Users can use more than one DS18B20 Sensor, but the sensor output is only connected to one Microcontroller pin. In addition, this sensor has waterproof properties [21]. So, this sensor can be used as a measuring instrument and for water heater control.

The degree of acidity or pH expresses the acidity or basicity a substance, solution, or object possesses. Normal pH has a value of 7, while a pH value > 7 indicates that the substance has base properties, and a pH value < 7 indicates acidity. pH 0 indicates a high degree of acidity, and pH 14 indicates the highest degree of basicity [22]. One way to find out the value of the degree of acidity is to use a pH sensor. An analog passive pH electrode connected to an embedded pH monitoring circuit supports UART and I2C communication protocols. It operates at a voltage range of 3.3-5.0 V and is compatible with any microprocessor that supports UART communication. This study was calibrated at 4.01, 7.01, and 10.01 to ensure accurate measurements [23].

One of the tools that can read the level of turbidity is a sensor that detects water turbidity by reading the optical properties of water due to light, and comparing the reflected light with the incident light [23]. Turbidity is a condition of water that is not clear and is caused by individual particles (suspended solids), which are generally invisible to the eye [24]. The more particles in the water, the higher the turbidity level of the water. A higher water turbidity level will be followed by a change in the sensor output voltage in turbidity sensors. The sensor utilizes an infrared LED as a light source and an infrared phototransistor to measure the amount of light that passes through the water. The resulting change in voltage is then converted into turbidity units, specifically NTU (Nephelometric Turbidity Units) [25].

The dissolved oxygen sensor in waterworks is used electrochemically to measure the amount of oxygen dissolved in water [26]. It uses the chemical reaction principle between oxygen and the electrolyte solution inside. When oxygen from water enters the sensor, it reacts with the electrolyte and produces an electrical signal [27]. This sensor works by being connected to a voltage source of 3.3 V to 5.0 V [23].

A relay is a switch that operates electrically and has two main parts: electromagnetic (coil) and mechanical (contact switch). Relay works by closing and opening the circuit with electric power through the coil. This relay is connected to the water pump and waterwheel for automatic handling [28]. The water pump is a component that moves water from one place to another using a drive [29]. The function of this waterwheel is to improve water quality as a source of dissolved oxygen levels in ponds [30]. To display information on this prototype, we need to use OLED. OLED (Organic Light-Emitting Diode) is an electronic component used as a display or monitor displaying data in characters, letters, numbers, and graphics. OLED technology was developed to obtain a comprehensive, flexible, inexpensive display that can be used efficiently for various display screen purposes [31]. It will be connected to a power supply as an energy source to activate this prototype. Power supply is equipment that supplies electricity to other equipment. The power supply in an electronic circuit requires direct current (DC) type power [32]. Commonly used power supplies include adapters and batteries as energy storage [33]

MQTT is a protocol designed by IBM with a publish/subscribe system that is suitable for Machine-to-Machine (M2M) based systems [16], [35]. Publishers use the publishing method to send messages on a specific topic. All clients who have subscribed to the same topic will receive the Publisher's published topic. Then, it will be sent through an intermediary called a broker, where the Publisher will send

data to the broker. Then, the data will be sent to the Subscriber, who has connected and adjusted the available topics [34]. MQTT provides significant flexibility to the framework and simplifies secure integration with cloud platforms, such as AWS, by utilizing certificates securely stored on the device via a crypto chip. Additionally, MQTT is employed to receive status updates from the intelligent object [35]. This study proposes an architecture that uses lightweight messaging protocols like MQTT to transmit sensor data and employs Node-Red as a data flow-based tool. Node-Red is a platform that provides several tools for creating an Internet of Things (IoT)- based system. The system built on the Node-Red platform uses several node components that form a flow [36].

The main component used in this research is the Mappi32 as a microcontroller. There is also power in the form of a 12 VDC adapter as a power supply for the microcontroller and water pump circuit. In addition, there are inputs from 5 sensors, namely the DFROBOOT Total Dissolved Solids Sensor, DS18B20, pH 4502C, DFROBOOT turbidity, and DFROBOOT Dissolved Oxygen. These sensors will be controlled and processed through Mappi32. Then, the sensor readings will be displayed on OLED. In addition, the results of sensor readings will also be displayed on the dashboard through a broker with the help of the internet that has been connected via Mappi32. If the reading results have a non-optimal category that exceeds the shrimp pond water quality standardization, activating the relay will send a signal. This is a water wheel to handle the results of non-optimal dissolved oxygen levels and a water pump to handle the results of salinity, temperature, pH, and turbidity. The design block diagram of the shrimp pond water quality monitoring system can be seen in Fig. 1.

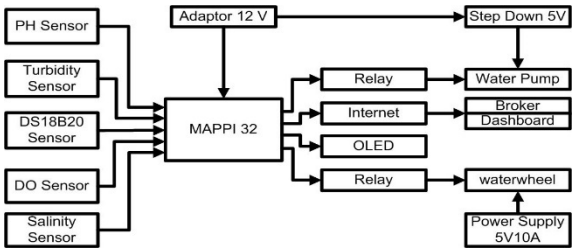

Fig. 1 Block Diagram of the Tool Design

Calibrate the sensors used in the designed tool system to validate the measured value against the value of conventional tools with standardization. One of the methods used in this calibration is the linear regression method. Linear regression is an analysis that studies the dependency relationship between one variable, called the dependent variable, and another variable, called the independent variable. Regression analysis can calculate the effect of changes in one variable on another. Linear regression can also form a relationship between independent and dependent variables.

Variable in a linear manner. This linear regression can be written through mathematical equations, such as equation 1 [37], [38].

$$Y = a + b \times x \tag{1}$$

with:

$$b = \frac{n \sum xy - \sum x \sum y}{n \sum x^2 - (\sum x)^2}$$

$$a = \frac{\sum y - b(\sum x)}{n}$$

From these two variables, the relationship can be seen based on the Coefficient of determination. The Coefficient of determination shows the extent to which the contribution of the independent variables in the regression model can explain the variation in the dependent variable. As for calculating The Coefficient of determination, it can be calculated using the correlation coefficient relationship. The correlation coefficient is a statistical measure that shows the extent to which two variables change together and how strong the linear relationship is between the two variables. The mathematical equation can be seen in equation 2.

$$R^2 = r^2 \tag{2}$$

with:

$$r = \frac{n \sum xy - \sum x \sum y}{\sqrt{(n \sum x^2 - (\sum x)^2)(n \sum y^2 - (\sum y)^2)}}$$

Description:
R = Coefficient of Determination
r = Correlation Coefficient
y = dependent variable (dependent variable)
x = independent variable (free variable)
a = constant
b = regression coefficient

Before calibrating, the error value of each experiment must be considered. A number, measurement, or calculation error is the numerical difference between the actual value and the value obtained from the given approach or calculation or measurement results. The error can be written mathematically in Equation 3 [39].

$$E = |a - a^*|$$

$$e = \frac{E}{a} = \frac{|a - a^*|}{a}$$

$$\xi a = e. 100\% \tag{3}$$

Description:
E = Absolute Error (Error)
a = Exact Value
a* = Approximate Value
e = Relative Error
ξa = Percentage Error (%)

III. Results and Discussion

TDS sensors are used to measure the amount of dissolved solids in water. One of these solids is salt. TDS Sensor Testing carried out in this study compares the value of the results measured on the conventional temperature measuring instruments and sensors, namely a Refractometer with a TDS Sensor DFROBOT. This sensor has three pins, namely VCC, Data, and GND. The TDS sensor has an output in the form of analog data, so it needs to be connected to the Mappi32 pin, which has an analog-to-digital (ADC) feature. The analog value read on Mappi32 is 12 bits (4095). The tools used in testing the TDS sensor can be seen in Fig 2.

Refractometers work by bending light. When light passes between two materials of different densities, such as water and air, it bends. The angle of this deflection depends on the difference in density between the two materials. A refractometer has a prism or lens that bends light. A liquid sample is placed on the surface of the prism or lens, and light passing through the sample will bend. The refractometer

measures this deflection angle and displays the result as a number indicating the refractive index of the liquid.

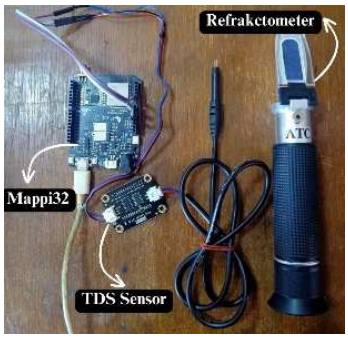

Fig. 2 TDS Sensor Testing Device

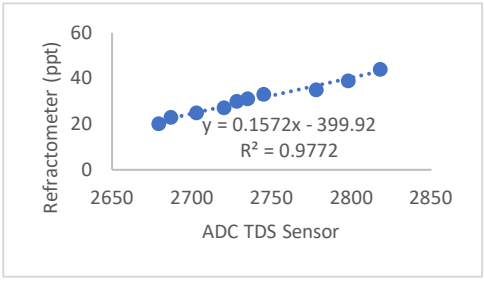

Fig. 3 TDS Sensor Linear Regression Visualization

Based on Fig. 3, the equation obtained in the linear regression equation y = 0.1572 x - 399.92 from 13 tested data points. Then, the equation will be entered into the Mappi32 programming to get a value that matches the actual salinity value. The Coefficient of determination in this TDS sensor test is 0.9772, which means that the closer to 1, the stronger the influence of the two variables will be. In addition, the Coefficient of variable x in the linear regression equation is positive, meaning that the higher the value of salt content read on the ADC of the TDS sensor, the higher the reading of the actual salt content value on the refractometer in units of ppt (parts per thousand). After entering the TDS Sensor calibration equation, data will be collected again with ten samples with different salt content levels. This measurement data will be analyzed based on the error and accuracy of each sample. This comparison can be seen in Table 1.

TABLE I
TDS SENSOR TESTING RESULTS AFTER CALIBRATION

No	TDS Sensor (ppt)	Refractometer (ppt)	Error (%)	Accuracy (%)
1	39.29	42	6.45	93.55
2	40.29	44	8.43	91.57
3	36.3	37	1.89	98.11
4	38.3	40	4.25	95.75
5	33.32	33	0.97	99.03
6	34.31	35	1.97	98.03
7	30.33	30	1.10	98.90
8	28.34	27	4.96	95.04
9	27.34	25	9.36	90.64
10	26.34	23	14.52	85.48
Average			5.39	94.61

Table 1 shows the latest test results after calibrating the TDS Sensor. These results obtained the average error and accuracy values of these 10 test samples of 5.39% and 94.61%, respectively.

The DS18B20 sensor can be used to measure the temperature of water. Testing the temperature sensor carried out in this study is to compare the value of the results measured on the sensor and conventional measuring instruments, namely mercury thermometers. This sensor has three pins, namely VCC, Data, and GND. The DS18B20 sensor has an output in the form of digital data. In this sensor circuit, a resistor is connected between the VCC Pin and the Data Pin, which prevents floating values in high conditions. The resistor is called a pull-up resistor with a value of 4.7Kohm. The tool used in testing the temperature sensor can be seen in Fig. 4.

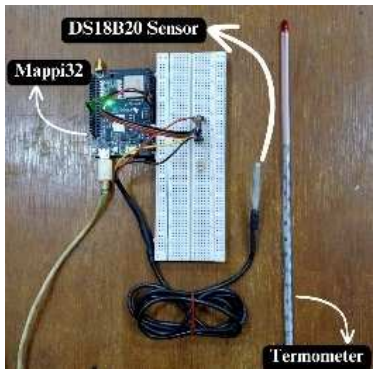

Fig. 4 Temperature Sensor Testing Device

Mercury thermometers operate on the principle of thermal expansion. As the temperature increases, the mercury in the glass tube expands and rises to a calibrated scale, indicating the temperature. Mercury was chosen because it has a stable thermal expansion and can accurately measure temperature over a wide range. As the temperature decreases, the mercury constricts and drops back down, giving consistent reading. Mercury also has a high boiling point and remains liquid across various temperatures, making it ideal for various applications. In addition, its uniform expansion properties ensure accurate reading. The visibility of mercury's silver color against the scale further aids accurate temperature measurement. However, mercury thermometers have declined due to their toxicity and have been replaced by safer alternatives.

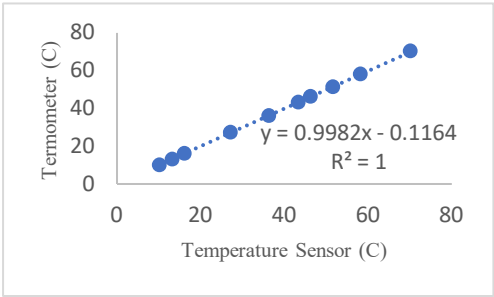

Fig. 5 Temperature Sensor Linear Regression Visualization

Based on Fig. 5, the linear regression equation y = 0.9982 x - 0.1164 was obtained from 10 tested data points. Then, the equation will be entered into the Mappi32 programming to get a value that matches the actual temperature value. The Coefficient of determination in this temperature sensor test is 1, which means that the closer to 1, the stronger the influence of the two variables will be. In addition, the Coefficient of

variable x in the linear regression equation is positive, meaning that the higher the temperature value read on the temperature sensor, the higher the actual temperature reading measured on the thermometer. After entering the temperature sensor calibration equation, data will be collected again with ten samples at different temperature levels. This measurement data will be analyzed based on the error and accuracy of each sample. This comparison can be seen in Table 2.

TABLE II
TEMPERATURE SENSOR TESTING RESULTS AFTER CALIBRATION

No	Thermometer (°C)	Temp Sensor (°C)	Error (%)	Accuracy (%)
1	35	35.01	0.03	99.97
2	36	36.13	0.36	99.64
3	37	37.07	0.19	99.81
4	47	47.05	0.11	99.89
5	49	49.04	0.08	99.92
6	50	50.04	0.08	99.92
7	53	53.1	0.19	99.81
8	57	57.06	0.11	99.89
9	60	60.09	0.15	99.85
10	69	68.95	0.07	99.93
Average			0.14	99.86

Table 2 shows the latest test results after calibrating the temperature sensor. These results obtained the average values of error and accuracy of these 10 test samples of 0.14% and 99.86%, respectively.

The pH 4502C sensor can be used to measure the acidity of water. The pH sensor testing in this study compares the value of the results measured on the sensor and conventional measuring instruments, namely the pH Meter. This sensor has three pins, namely VCC, Data, and GND. The pH sensor has an output in analog data, so it needs to be connected to the Mappi32 pin, which has an Analog Digital (ADC) feature. The analog value read on Mappi32 is 12 bits (4095). The tool used in testing the pH sensor can be seen in Fig. 6.

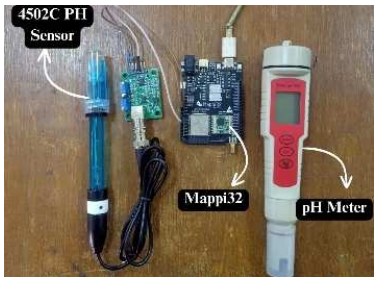

Fig. 6 pH Sensor Testing Device

pH meters measure the activity of hydrogen ions (H+) in a solution to determine its acidity or basicity. This tool has a glass electrode that is sensitive to H + ions. When the electrode is dipped into a solution, the H+ ions in the solution interact with the surface of the electrode, producing an electrical voltage. The pH meter measures this voltage and converts it to a pH value displayed on the screen. The pH value indicates how acidic or alkaline a solution is, with a scale from 0 (very acidic) to 14 (very basic), and 7 (neutral).

Based on Fig. 7, the equation obtained in the linear regression equation y = -0.0046x + 19.931 from 14 tested data points. Then, the equation will be entered into the Mappi32 programming to get a value that matches the actual pH value. The Coefficient of determination in this pH sensor test is 0.9968, which means that the closer to 1, the stronger the influence of the two variables will be. In addition, the Coefficient of variable x in the linear regression equation is negative, meaning that the lower the ADC value of the pH sensor, the higher the pH value in a solution measured by the pH meter.

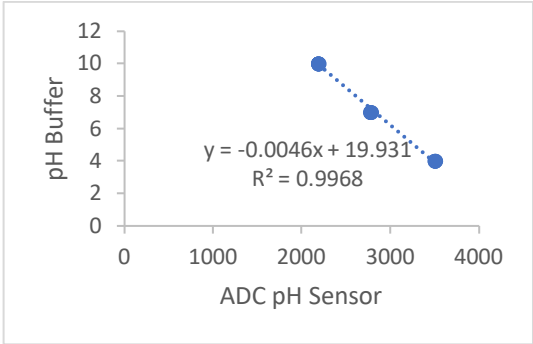

Fig. 7 pH Sensor Linear Regression Visualization

After entering the pH sensor calibration equation, data will be collected again with twelve samples with different acidity levels. This measurement data will be analyzed based on the results of each sample's error and accuracy. This comparison can be seen in Table 3.

TABLE III
PH SENSOR TESTING RESULTS AFTER CALIBRATION

No	pH Meter	pH Sensor	Error (%)	Accuracy (%)
1	3.98	4.09	2.76	97.24
2	6.69	6.95	3.89	96.11
3	6.8	7.03	3.38	96.62
4	6.99	7.26	386	96.14
5	7.12	7.36	3.37	96.63
6	7.14	7.5	5.04	94.96
7	7.16	7.4	3.35	96.65
8	7.19	7.24	0.70	99.30
9	7.25	7.62	5.10	94.90
10	8.02	7.85	2.12	97.88
11	9.97	9.93	0.40	99.60
12	9.99	9.97	0.20	99.80
Average			2.85	97.15

Table 3 shows the latest test results obtained after calibrating the pH sensor. These results obtained the average error and accuracy values of these 12 test samples of 2.85% and 97.15%, respectively.

The DFRobot Turbidity Sensor can be used to measure turbidity in water. Turbidity sensor testing carried out in this study is to compare the value of the results measured on the sensor and conventional measuring instruments, namely, turbidity meters. The turbidity sensor has an output in the form of analog data, so it needs to be connected to the Mappi32 pin, which has an analog-to-digital (ADC) feature. The analog pin read on the Mappi32 is 12 bits (4095). The turbidity sensor test produces fluctuating ADC data. This happens because the working principle of this sensor is light refraction, which means that this sensor is susceptible to the presence of light shining on the water sample. Therefore, a solution was made to make a cover from a pipe that covers

this sensor. The tool used in testing the turbidity sensor can be seen in Fig. 8.

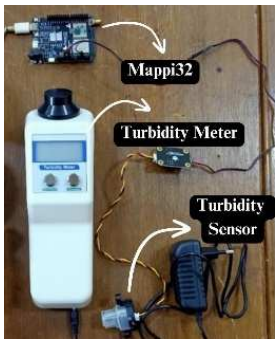

Fig. 8 Turbidity Sensor Testing Device

Turbidity meters measure the amount of light scattered by suspended particles in a liquid. It emits a light beam into the water sample through a light source, usually a lamp or laser. The particles in the water will scatter the light. The sensor in the turbidity meter then detects the intensity of the scattered light. The more particles in the water, the higher the intensity of the scattered light, which means the turbidity or cloudiness of the water is higher. The results of this measurement are usually displayed in NTU (Nephelometric Turbidity Units).

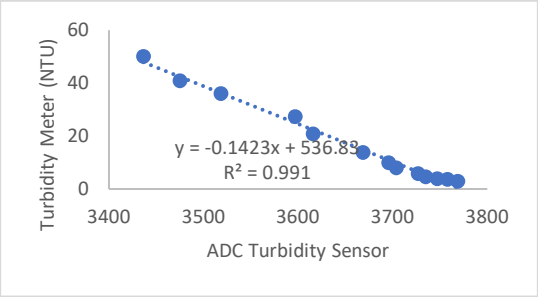

Fig. 9 Turbidity Sensor Linear Regression Visualization

Based on Fig. 9, the linear regression equation y = -0.1423x + 536.83 from 13 tested data points will be entered into Mappi32 programming to get a value that matches the actual turbidity value. The Coefficient of determination in this turbidity sensor test is 0.991, which means that the closer to 1, the stronger the influence of the two variables will be.

TABLE IV
NIGHTTIME TURBIDITY SENSOR TEST RESULTS AFTER CALIBRATION

No	Turbidity Meter (NTU)	Turbidity Sensor (NTU)	Error (%)	Accuracy (%)
1	5.5	5.75	4.55	95.45
2	5.9	5.61	4,92	95.08
3	6.5	6.79	4,46	95.54
4	7.6	7.83	3,03	96.97
5	12.4	12.61	1,69	98.31
6	13.5	12.3	8,89	91.11
7	14.2	13.56	4,51	95.49
8	15.5	14.73	4,97	95.03
9	16	15.39	3,81	96.19
10	18.9	18.07	4,39	95.61
11	19.7	18.94	3,86	96.14
12	22.93	23.5	2,49	97.51
13	23.45	24.5	4,48	95.52
Average			4,31	95.69

In addition, the Coefficient of variable x in the linear regression equation is negative, meaning that the lower the ADC value of the turbidity sensor that is read on, the higher the actual turbidity reading of a solution measured by the turbidity meter. After entering the turbidity sensor calibration equation, data will be collected again with 13 samples with different turbidity levels and taken during day and night conditions. This measurement data will be analyzed based on the results of each sample's error and accuracy. This comparison can be seen in Table 4. Table 4 shows the latest test results after calibrating the turbidity sensor, which was carried out at night. These results obtained the average error and accuracy of these thirteen test samples of 4.31% and 95.69%, respectively.

Based on Table 5, the latest test results were obtained after calibrating the turbidity sensor during the day. These results obtained the average error and accuracy of these 13 test samples of 5,97% and 94.03%. Therefore, the error and accuracy obtained through the turbidity sensor testing process are 5.14% and 94.86%.

TABLE V
DAYTIME TURBIDITY SENSOR TEST RESULTS AFTER CALIBRATION

No	Turbidity Meter (NTU)	Turbidity Sensor (NTU)	Error (%)	Accuracy (%)
1	12	10.86	9.50	90.50
2	12.5	13.12	4.96	95.04
No	**Turbidity Meter (NTU)**	**Turbidity Sensor (NTU)**	**Error (%)**	**Accuracy (%)**
3	13	13.6	4.62	95.38
4	13.5	14.95	10.74	89.26
5	13.8	13.56	1.74	98.26
6	14	15.24	8.86	91.14
7	14.5	15.82	9.10	90.90
8	15	15.47	3.13	96.87
9	15.3	16.68	9.02	90.98
10	15.8	16.51	4.49	95.51
11	16	16.34	2.13	97.88
12	17.5	16.86	3.66	96.34
13	18.6	17.55	5.65	94.35
Average			5.97	94.03

The DFRobot dissolved oxygen sensor can measure dissolved oxygen levels in water. The dissolved oxygen sensor testing in this study compares the value of the results measured on the sensor with those of conventional measuring instruments, namely dissolved oxygen meters. This sensor has three pins, namely VCC, Data, and GND. The DO sensor has an output in analog data, so it needs to be connected to the Mappi32 pin, which has an analog-to-digital (ADC) feature. The analog pin read on the Mappi32 is 12 bits (4095). The tool used in testing the turbidity sensor can be seen in Fig. 10.

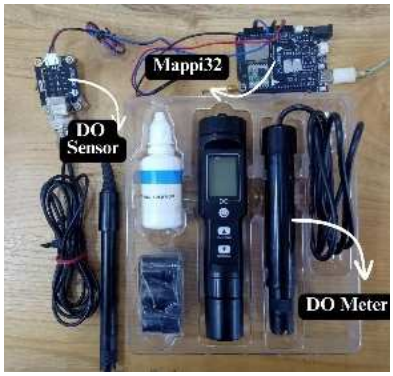

Fig. 10 Turbidity Sensor Testing Device

Dissolved oxygen meters (DO meters) measure the amount of oxygen dissolved in water. This tool generally uses an oxygen electrode consisting of a cathode and an anode submerged in an electrolyte and separated from the water sample by an oxygen-permeable membrane. When an electric current is applied, oxygen penetrating the membrane reacts at the cathode, producing an electric current proportional to the dissolved oxygen concentration. The DO meter then measures this electric current and converts it to an oxygen concentration value displayed on the screen, usually in mg/L (milligrams per liter).

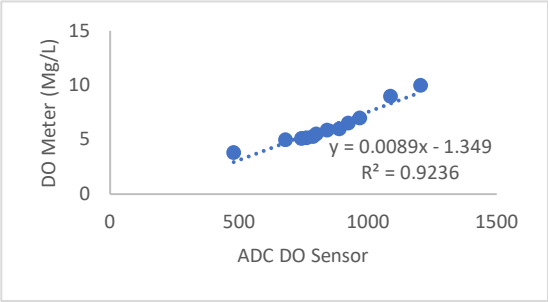

Fig. 11 DO Sensor Linear Regression Visualization

Based on Fig 11, the equation obtained in the linear regression equation y = 0.0089x - 1.349 from 12 tested data. Then, the equation will be entered into Mappi32 programming to get a value that matches the actual turbidity value. The Coefficient of determination in this pH sensor test is 0.9236, which means that the closer to 1, the stronger the influence of the two variables will be. In addition, the Coefficient of variable x in the linear regression equation is positive, meaning that the higher the oxygen levels read on the DO sensor, the higher the reading of the actual oxygen levels measured on the DO Meter. After entering the dissolved oxygen sensor calibration equation, data will be collected again with 14 samples with different oxygen levels. This measurement data will be analyzed based on the error and accuracy of each sample. This comparison can be seen in Table 6.

TABLE VI
DO SENSOR TESTING RESULTS AFTER CALIBRATION

No	DO Meter (Mg/L)	DO Sensor (Mg/L)	Error (%)	Accuracy (%)
1	6.1	5.82	4.59	95.41
2	6.1	4.94	19.02	80.98
3	6.1	5.96	2.30	97.70
4	6.1	6.27	2.79	97.21
5	6	5.82	3.00	97.00
6	6	6.78	13.00	87.00
7	6	5.25	12.50	87.50
8	6	5.44	9.33	90.67
9	6	5.02	16.33	83.67
10	6	6.63	10.50	89.50
11	4.5	4.86	8.00	92.00
12	4.5	5.07	12.67	87.33
13	4.5	4.68	4.00	96.00
14	4.5	4.76	5.78	94.22
Average			8.84	91.16

Table 6. shows the latest test results after calibrating the dissolved oxygen sensor. These results show that the average error and accuracy of the 14 test data are 9.67% and 90.33%, respectively.

The monitoring device consists of sensor components that send parameter readings of salinity, temperature, pH, turbidity, and oxygen levels to the Node-Red dashboard. When the readings from these sensors exceed the standardization of shrimp pond water quality parameters, the wheel or water pump will automatically activate to handle and restore the parameter value to the optimal value. The packaged tool can be seen in Fig. 12.

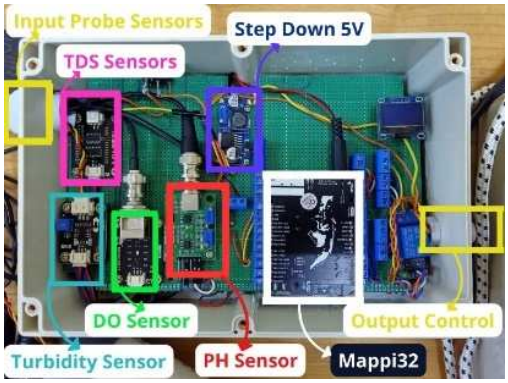

Fig. 12 Results of Shrimp Pond Water Quality Monitoring Device

Shrimp pond water conditions have > 4 Mg / L standardized oxygen levels. Therefore, the value read on the DO sensor is said to be not optimal when it is < 4 Mg / L. Therefore, the value read on the DO sensor is said to be not optimal when it is <4 Mg/L. To overcome the non-optimality of the DO value read, automatic handling is made when the DO value is less than the standardization set. This automatic handling increases dissolved oxygen levels in the shrimp pond water. The modeling circuit of this mill can be seen in Fig. 13. This pinwheel model is composed of several key components: a 5V 10A power supply, a 12V 3A DC motor, a dimmer module to control the motor's rotation speed to prevent water from splashing out of the research medium, and a relay that acts as an automatic switch.

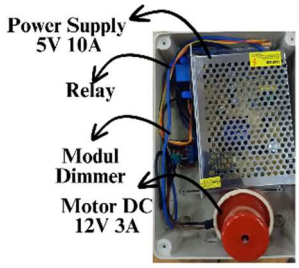

Fig. 13 Waterwheel Modeling Circuit

As shown in Fig. 13, the waterwheel can return oxygen levels to the optimal value of > 4 Mg / L. The data displayed in Fig. 14 is a sample of dissolved oxygen levels at a critical point, namely <4 Mg/L. The data is quoted from the measurement data in the morning, a crisis time condition with the lowest oxygen content and the highest carbon dioxide value. Therefore, morning is a condition that needs to be considered when monitoring the water quality of shrimp ponds.

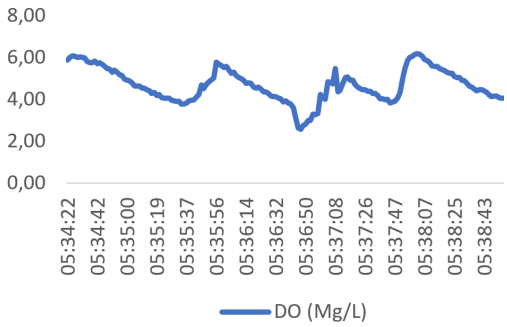

Fig. 14 Change in DO value due to waterwheel automation

Shrimp pond water conditions have standardized values of temperature 26-32 °C, salinity 30-35 ppt, pH 7.6-8.3, and turbidity value 11 - 24 NTU. Therefore, the value read on the sensors is more than the standardized optimal point, so it is said that the water quality parameters of shrimp ponds are unsuitable for shrimp breeding. To overcome this non-optimality, automatic handling is made when the parameters of temperature, salinity, pH, and turbidity exceed the predetermined standardization. This automatic handling aims to restore or reduce the reading of the four parameters by adding water automatically with a water pump.

Based on Fig. 15, the pH parameter sample has a value that is not optimal because of the treatment, namely the addition of detergent solution, to see the response of the automatic handling that has been made. The sample in Fig. 29 states that adding water automatically reduces the pH parameter to below 8.3, the optimal pH threshold for shrimp pond water quality. The water pump will activate when the pH sensor measurement value is more significant than 8.3.

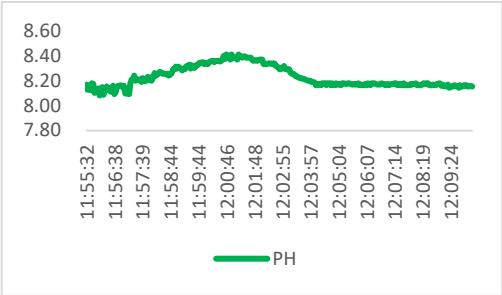

Fig. 15 pH value changes due to water pump automation

Based on Fig. 16, the salinity parameter sample has a value that is not optimal because of the treatment, namely, the addition of salt solution to see the response of automatic handling that has been made, namely, water pump automation. The sample in Fig. 30 states that adding water can automatically reduce the salinity parameter to below 35 ppt, the optimal salinity threshold for shrimp pond water quality. This research has been integrated with the Internet of Things, so the system can run with the help of the Internet and be monitored in real-time through the dashboard of the Node-Red platform. As a distributor of information in this system, an MQTT broker connected between the mappi32 microcontroller and Node-Red makes this dashboard.

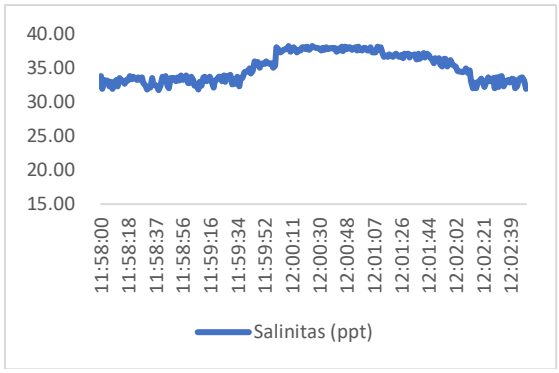

Fig. 16 Salinity value changes due to water pump automation

Based on Fig. 17, the first node used is MQTT IN, which can subscribe to the data that the sensors send to the selected MQTT server. The MQTT server used in this research is HIVEMQ with the server https://broker.mqtt-dashboard.com/. Previously, data from each sensor used would be sent to the server. The second node, the gauge node, will provide needle-like instructions about the value read on the sensor. The third node, the chart node, is a node that is used to function as an accumulator of sensors that have been read. Then, this node will display the data sent and store it temporarily. Thus, the trend of value changes can be seen clearly.

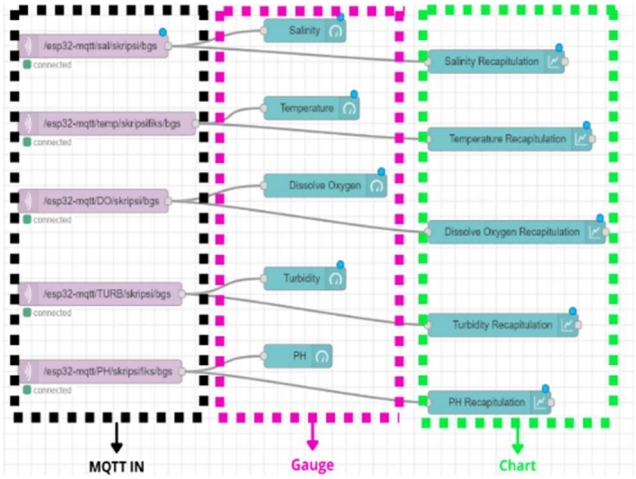

Fig. 17 Red node workflow used

On MQTT in Node, Mappi32 will take data, separate the data, and adjust the data from the sensors on the Gauge Node, then send it to the MQTT Server used, namely HIVEMQ (https://broker.mqtt-dashboard.com/). In Figure 17, the data collected from the Gauge Node are salinity, temperature, oxygen level, turbidity, and pH data. When the data has been taken, separated, and adjusted to the MQTT In Node, it then goes to the Chart Node, which will display and temporarily store the data sent to the server.

Based on the workflow in Fig. 17, a simple dashboard can display data from sensor readings. The data the sensors have read will be sent through the MQTT broker, which is represented through this dashboard. The dashboard can be seen in Fig. 18.

Fig. 18 Red node workflow used

The transmission latency data will be tested after the dashboard is successfully connected to the monitoring system. Latency testing on the Internet of Things (IoT) system is carried out to determine the delay in sending data from sensors' readings to the MQTT server. This test compares the time of sending data from the sensor sent on the Arduino IDE serial monitor with the time received by the MQTT broker, mqtt-dashboard.com. This latency test uses a website used in the testing process, client-cloud.mqtt.cool.

It is based on Fig. 19. The latency testing on the MQTT server broker.mqtt-dashboard.com shows an average latency value of 593.3 ms from 20 test data. Of the 20-test data, the worst test result value was obtained with a latency value of 671 ms, and the best test result value with a latency value of 522 ms. This latency value indicates that there is a delay in the process of sending sensor reading data to the Internet of Things support server. The internet speed during the testing process is one factor that affects the latency value.

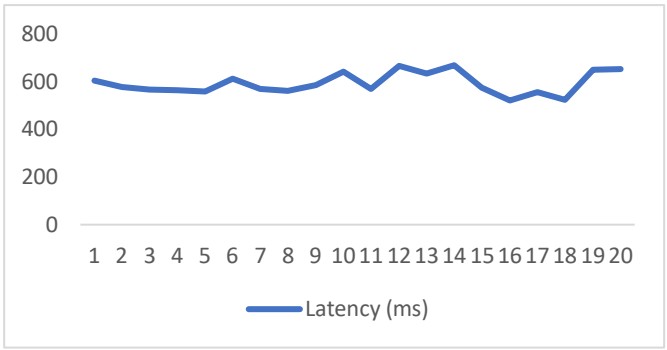

Fig. 19 MQTT protocol latency testing

Figure 20 is a recapitulation of the average values at 05.00-07.00 a.m., afternoon at 12.00-02.00 p.m., and evening at 07.00-09.00 p.m. for 10 days of monitoring. The monitoring results concluded that when the temperature is coldest or in the morning (27,13 °C), pH (7,66) and Dissolved Oxygen (5,22 Mg/L) obtained will be the lowest. Meanwhile, for the highest temperatures during the day (27,41 °C), pH (7,84) of the water and Dissolved Oxygen (5,54 Mg/L) obtained will be the highest. Meanwhile, salinity is inversely proportional to temperature. This means that the higher the temperature measured, the lower the salinity obtained. The Turbidity value does not affect temperature but depends on the presence of sunlight. Therefore, the results of the turnover value experience are different only at night, the values in the morning and during the day are the same.

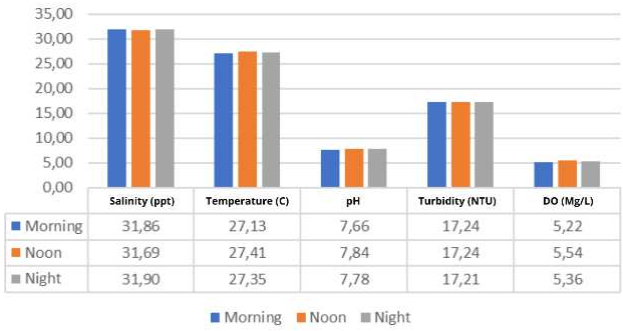

	Salinity (ppt)	Temperature (C)	pH	Turbidity (NTU)	DO (Mg/L)
Morning	31,86	27,13	7,66	17,24	5,22
Noon	31,69	27,41	7,84	17,24	5,54
Night	31,90	27,35	7,78	17,21	5,36

Fig. 20 Recapitulation of Shrimp Pond Quality Monitoring

IV. Conclusion

The shrimp pond water quality monitoring tool with Mappi32 has been realized, and the error value read on the sensors from the testing process is 5.39% TDS sensor, 0.14% temperature sensor, 2.85% pH sensor, 5.14% turbidity sensor, and 9.67% DO sensor. Real-time monitoring of shrimp pond water quality has been realized, and it can be monitored through the Node-Red dashboard using the IoT Message Queuing Telemetry Transport (MQTT) protocol with an average latency value of 593.3 ms. Based on the monitoring data obtained, the average value of parameters for ten days in the morning salinity 31.86 ppt; temperature 27.13 C; pH 7.66; turbidity 17.24 NTU; and dissolved oxygen 5.22 Mg/L; in the afternoon salinity 31.69 ppt; temperature 27.41 C; pH 7.84; turbidity 17.24 NTU; and dissolved oxygen 5.54 Mg/L; and at night salinity 31.90 ppt; temperature 27.35 C; pH 7.78; turbidity 17.21 NTU; and dissolved oxygen 5.36 Mg/L.

The ability to communicate data is the potential scalability factor when implementing this IoT-based monitoring system in larger-scale shrimp farming operations. Because, based on the data obtained, the value of data latitude or delay is up to 671 ms. The data latency or delay will increase if this is done on a large scale with inaccurate pond area calculations and microcontroller placement calculations. Because of this, the author suggests that a method, such as the Fuzzy Logic method, is needed to determine the optimal status of shrimp pond water with five parameters simultaneously and discuss the optimality and effectiveness of the method's influence on the control system. In addition, a mini-PC such as a Raspberry Pi is needed to make it easier to store data and observe so that the Internet of Things system can be stored online.

References

[1] J. Malisan, E. Marpaung, G. Hutapea, F. S. Puriningsih, and D. Arianto, "Development of short sea shipping in the north coast of Java Island, Indonesia as a potential market," *Transp. Res. Interdiscip. Perspect.*, vol. 18, no. January, p. 100760, 2023, doi: 10.1016/j.trip.2023.100760.

[2] R. Arifin, M. Hanita, and A. J. S. Runturambi, "Maritime border formalities, facilitation and security nexus: Reconstructing immigration clearance in Indonesia," *Mar. Policy*, vol. 163, no. June 2023, 2024, doi: 10.1016/j.marpol.2024.106101.

[3] E. Djunarsjah, A. P. Putra, D. Kusumadewi, K. Yudistira, and M. M. Julian, "The Concept of Integration between State and Provincial Sea Boundaries in Indonesia," *Sustain.*, vol. 14, no. 3, 2022, doi:10.3390/su14031659.

[4] M. Asmild, V. Hukom, R. Nielsen, and M. Nielsen, "Is economies of scale driving the development in shrimp farming from Penaeus monodon to Litopenaeus vannamei? The case of Indonesia," *Aquaculture*, vol. 579, no. January 2023, p. 740178, 2024, doi:10.1016/j.aquaculture.2023.740178.

[5] A. Mustafa *et al.*, "Strategy for Developing Whiteleg Shrimp (Litopenaeus vannamei) Culture Using Intensive/Super-Intensive Technology in Indonesia," *Sustain.*, vol. 15, no. 3, 2023, doi:10.3390/su15031753.

[6] A. Mustafa *et al.*, "Temporal and Spatial Analysis of Coastal Water Quality to Support Application of Whiteleg Shrimp Litopenaeus vannamei Intensive Pond Technology," *Sustain.*, vol. 14, no. 5, 2022, doi: 10.3390/su14052659.

[7] M. Manoj, V. D. Kumar, M. Arif, E. R. Bulai, P. Bulai, and O. Geman, "State of the Art Techniques for Water Quality Monitoring Systems for Fish Ponds Using IoT and Underwater Sensors: A Review," *Sensors*, vol. 22, no. 6, 2022, doi: 10.3390/s22062088.

[8] Y. Xue, L. Li, S. Dong, Q. Gao, and X. Tian, "The effects of different carbon sources on the production environment and breeding parameters of litopenaeus vannamei," *Water (Switzerland)*, vol. 13, no. 24, pp. 1–16, 2021, doi: 10.3390/w13243584.

[9] Z. Song, C. Liu, Y. Luan, Y. Qi, and A. Xu, "Effect of Zero Water Exchange Systems for Litopenaeus vannamei Using Sponge Biocarriers to Control Inorganic Nitrogen and Suspended Solids Simultaneously," *Sustain.* , vol. 15, no. 2, 2023, doi:10.3390/su15021271.

[10] M. M. Hemal *et al.*, "An Integrated Smart Pond Water Quality Monitoring and Fish Farming Recommendation Aquabot System," *Sensors*, vol. 24, no. 11, pp. 1–22, 2024, doi:10.3390/s24113682.

[11] S. B. W. A. C. Ministry Of Marine Affairs And Fisheries Directorate General Of Aquaculture, *Cultivation of Vaname Shrimp (Litopenaeus Vannamei) in Millennial Ponds*. Situbondo, 2021.

[12] R. Wiryasaputra, C. Y. Huang, Y. J. Lin, and C. T. Yang, "An IoT Real-Time Potable Water Quality Monitoring and Prediction Model Based on Cloud Computing Architecture," *Sensors*, vol. 24, no. 4, pp. 1–13, 2024, doi: 10.3390/s24041180.

[13] B. L. Risteska Stojkoska and K. V. Trivodaliev, "A review of Internet of Things for smart home: Challenges and solutions," Journal of Cleaner Production, vol. 140, pp. 1454–1464, Jan. 2017, doi: 10.1016/j.jclepro.2016.10.006.

[14] P. Cofta, K. Karatzas, and C. Orłowski, "A conceptual model of measurement uncertainty in IoT sensor networks," *Sensors*, vol. 21, no. 5, pp. 1–19, 2021, doi: 10.3390/s21051827.

[15] S. Tian and V. G. Vassilakis, "On the Efficiency of a Lightweight Authentication and Privacy Preservation Scheme for MQTT," *Electron.*, vol. 12, no. 14, 2023, doi: 10.3390/electronics12143085.

[16] B. Mishra and A. Kertesz, "The use of MQTT in M2M and IoT systems: A survey," *IEEE Access*, vol. 8, pp. 201071–201086, 2020, doi: 10.1109/access.2020.3035849.

[17] J. Simla. A, R. Chakravarthy, and M. Leo. L, "An Experimental study of IoT-Based Topologies on MQTT protocol for Agriculture Intrusion Detection," *Measurement: Sensors*, vol. 24, p. 100470, Dec. 2022, doi:10.1016/j.measen.2022.100470.

[18] H. J. Jara Ochoa, R. Peña, Y. Ledo Mezquita, E. Gonzalez, and S. Camacho-Leon, "Comparative Analysis of Power Consumption between MQTT and HTTP Protocols in an IoT Platform Designed and Implemented for Remote Real-Time Monitoring of Long-Term Cold Chain Transport Operations," *Sensors*, vol. 23, no. 10, 2023, doi:10.3390/s23104896.

[19] R. Bogdan, C. Paliuc, M. Crisan-Vida, S. Nimara, and D. Barmayoun, "Low-Cost Internet-of-Things Water-Quality Monitoring System for Rural Areas," *Sensors*, vol. 23, no. 8, 2023, doi: 10.3390/s23083919.

[20] K. Koritsoglou et al., "Improving the Accuracy of Low-Cost Sensor Measurements for Freezer Automation," *Sensors*, vol. 20, no. 21, p. 6389, Nov. 2020, doi: 10.3390/s20216389.

[21] I. Guevara, S. Ryan, A. Singh, C. Brandon, and T. Margaria, "Edge IoT Prototyping Using Model-Driven Representations: A Use Case for Smart Agriculture," *Sensors*, vol. 24, no. 2, p. 495, Jan. 2024, doi: 10.3390/s24020495.

[22] R. Wiryasaputra, C.-Y. Huang, Y.-J. Lin, and C.-T. Yang, "An IoT Real-Time Potable Water Quality Monitoring and Prediction Model Based on Cloud Computing Architecture," *Sensors*, vol. 24, no. 4, p. 1180, Feb. 2024, doi: 10.3390/s24041180.

[23] R. A. Bórquez López, L. R. Martinez Cordova, J. C. Gil Nuñez, J. R. Gonzalez Galaviz, J. C. Ibarra Gamez, and R. Casillas Hernandez, "Implementation and Evaluation of Open-Source Hardware to Monitor Water Quality in Precision Aquaculture," *Sensors*, vol. 20, no. 21, p. 6112, Oct. 2020, doi: 10.3390/s20216112.

[24] B. Lednicka et al., "Water Turbidity and Suspended Particulate Matter Concentration at Dredged Material Dumping Sites in the Southern Baltic," *Sensors*, vol. 22, no. 20, p. 8049, Oct. 2022, doi:10.3390/s22208049.

[25] M. Naloufi et al., "Long-Term Stability of Low-Cost IoT System for Monitoring Water Quality in Urban Rivers," *Water*, vol. 16, no. 12, p. 1708, Jun. 2024, doi: 10.3390/w16121708.

[26] G. M. e Silva, D. F. Campos, J. A. T. Brasil, M. Tremblay, E. M. Mendiondo, and F. Ghiglieno, "Advances in Technological Research for Online and In Situ Water Quality Monitoring—A Review," *Sustainability*, vol. 14, no. 9, p. 5059, Apr. 2022, doi:10.3390/su14095059.

[27] M. Siddika, Md. M. Hasan, T. A. Oyshi, and M. A. Hasnat, "Electrocatalytic Reduction of O2 by ITO-IrOx: Implication for Dissolved Oxygen Sensor in the Alkaline Medium," *Electrochem*, vol. 4, no. 2, pp. 145–155, Mar. 2023, doi: 10.3390/electrochem4020012.

[28] K. Zhou, J. Xiao, H. Zhuo, Y. Mo, D. Zhang, and P. Du, "Optimization of the Relay Coil Compensation Capacitor for the Three-Coil Wireless Power Transmission System," *Sustainability*, vol. 15, no. 20, p. 15094, Oct. 2023, doi: 10.3390/su152015094.

[29] F. Jan, N. Min-Allah, S. Saeed, S. Z. Iqbal, and R. Ahmed, "IoT-Based Solutions to Monitor Water Level, Leakage, and Motor Control for Smart Water Tanks," *Water*, vol. 14, no. 3, p. 309, Jan. 2022, doi:10.3390/w14030309.

[30] C. Tong, K. He, and H. Hu, "Design and Application of New Aeration Device Based on Recirculating Aquaculture System," *Applied Sciences*, vol. 14, no. 8, p. 3401, Apr. 2024, doi: 10.3390/app14083401.

[31] S. Naqvi et al., "Unraveling Degradation Processes and Strategies for Enhancing Reliability in Organic Light-Emitting Diodes," *Nanomaterials*, vol. 13, no. 23, p. 3020, Nov. 2023, doi: 10.3390/nano13233020.

[32] V. Vossos *et al.*, "Adoption Pathways for DC Power Distribution in Buildings," *Energies (Switzerland)*, vol. 15, no. 3, 2022, doi:10.3390/en15030786.

[33] Z. Tsiropoulos, I. Gravalos, E. Skoubris, V. Poulek, T. Petrík, and M. Libra, "A Comparative Analysis Between Battery- and Solar-Powered Wireless Sensors for Soil Water Monitoring," *Appl. Sci.*, vol. 12, no. 3, 2022, doi: 10.3390/app12031130.

[34] A. Manowska, A. Wycisk, A. Nowrot, and J. Pielot, "The Use of the MQTT Protocol in Measurement, Monitoring and Control Systems as Part of the Implementation of Energy Management Systems," *Electron.*, vol. 12, no. 1, 2023, doi: 10.3390/electronics12010017.

[35] M. Esposito, A. Belli, L. Palma, and P. Pierleoni, "Design and Implementation of a Framework for Smart Home Automation Based on Cellular IoT, MQTT, and Serverless Functions," *Sensors*, vol. 23, no. 9, p. 4459, May 2023, doi: 10.3390/s23094459.

[36] A. Medina-Pérez, D. Sánchez-Rodríguez, and I. Alonso-González, "An internet of thing architecture based on message queuing telemetry transport protocol and node-red: A case study for monitoring radon gas," *Smart Cities*, vol. 4, no. 2, pp. 803–818, 2021, doi:10.3390/smartcities4020041.

[37] H. Y. Chen and C. Chen, "Evaluation of Calibration Equations by Using Regression Analysis: An Example of Chemical Analysis," *Sensors*, vol. 22, no. 2, p. 447, Jan. 2022, doi: 10.3390/s22020447.

[38] D. Sengupta, "Linear Models in Statistics," *Journal of the American Statistical Association*, vol. 96, no. 455, pp. 1138–1138, Sep. 2001, doi:10.1198/jasa.2001.s414.

[39] L. D. Mejía-Ferreyra, L. García-Romero, S. T. Sánchez-Quispe, J. Apolinar-Cortés, and J. C. Orantes-Avalos, "Automatic Rainwater Quality Monitoring System Using Low-Cost Technology," *Water*, vol. 16, no. 12, p. 1735, Jun. 2024, doi: 10.3390/w16121735.